

Phase transitions in homogeneous biopolymers: basic concepts and methods. *

N. Theodorakopoulos [†]

*Theoretical and Physical Chemistry Institute,
National Hellenic Research Foundation,
Vasileos Constantinou 48, 116 35 Athens, Greece*

February 1, 2008

The basic models of helix-coil transitions in biomolecules are introduced. These include phenomenological, zipper (Bragg-Zimm) models of polypeptides, loop-entropy (Poland-Scheraga) and Hamiltonian (Peyrard-Bishop) models of homogeneous DNA denaturation. The transfer integral approach to one-dimensional thermodynamics is presented in some detail, including the necessary extensions to deal with the singular integral equations arising in the case of on-site potentials with a flat top. The (non-)applicability of the theorems which prohibit phase transitions in one-dimensional systems is discussed.

1 Introduction

The purpose of these notes is to provide a brief introduction to concepts and methods employed in the description of thermodynamic phase transitions in model biomolecular systems. This is one of the areas where the LOCNET network has been active, with an emphasis on modelling the fundamental interactions which provide a basis for understanding both the cooperative behavior and the nonlinear dynamics (what I will call “Hamiltonian” models). My primary aim is therefore to present a working introduction to this area, including some necessary details on methods and tools; I hope that young researchers who enter the field will find this material useful.

On the other hand there is a long and distinguished tradition in the field, which has achieved remarkable progress, based on a phenomenological de-

*Proceedings of the conference on “*LOCALIZATION AND ENERGY TRANSFER IN NONLINEAR SYSTEMS*”, June 17-21, 2002, San Lorenzo de El Escorial, Madrid, Spain. To be published by World Scientific.

[†]Work partially supported by EU contract HPRN-CT-1999-00163 (LOCNET network).

scription of the statistical properties of helix formation and growth and the entropies associated with them. I have therefore chosen to include a section on fundamentals of these “zipper” and “loop”-based models[1]. Again, the hope is that researchers who are active in developing microscopic Hamiltonian models will be guided by the succesful features of phenomenological, “zipper” and “loop” models. In addition, there is a simple, utilitarian reason for doing this: most of the experimental data presently available has been analyzed, directly or indirectly, in terms of such models. Therefore, anyone seriously interested in comparing theory and experiment should be familiar with them.

The plan of this review is as follows: Section 2 deals with zipper and loop models of polypeptides and DNA, respectively. Section 3 describes the Hamiltonian approach to DNA denaturation, including a somewhat detailed introduction to the transfer integral method. An appendix discusses the (non-)applicability of theorems which prohibit phase transitions in one dimension to the models presented.

2 Zippers and Loops

2.1 Helix-Coil transitions in polypeptides

2.1.1 Background

Synthetic polypeptides, i.e. macromolecules consisting of identical amino-acid residues, are ideal for studying the transition from the alpha-helical to coil-like structure. Understanding of this transition is central to controlling the stability of secondary protein structure[2]. Residues in helical regions give rise to distinct experimental signatures (e.g. viscosity, optical rotation). At a given macromolecular size N - which can be controlled in synthetic polypeptides - one can measure the helix fraction as a function of temperature. Typically[3], that fraction completes the transition from 1 to 0 over a fairly narrow temperature range - a few degrees K in the case of long chains. Chemists describe the process $A(helix) \longleftrightarrow B(coil)$ as an equilibrium between the two species,

$$K \equiv \frac{c_B}{c_A} \equiv e^{-\Delta G/T} \quad (1)$$

where the helix fraction is given by

$$\Theta \equiv \frac{c_A}{c_A + c_B} = \frac{1}{1 + K} . \quad (2)$$

The sign convention is as follows: I am looking at the conversion of helix (A) to coil (B); therefore $\Delta G = G_B - G_A = \Delta H - T\Delta S$, and $\Delta H > 0$, i.e. the helix is energetically favored.

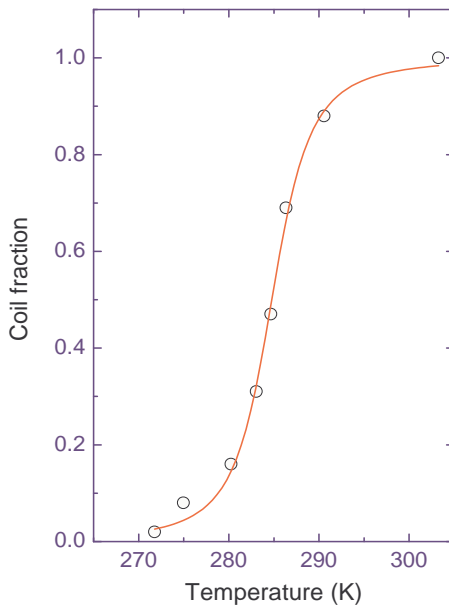


Figure 1: Coil fraction vs. temperature for a polypeptide (poly- γ -benzyl-L-glutamate) of controlled ($N = 1500$) length; The curve has been calculated in the framework of the generalized zipper model - cf. Eq. 16 below - (redrawn after Ref. [3]).

The value $\Theta = 0.5$ defines the midpoint of the transition, T_m . Assuming (although this is not exact, and sometimes not even a good approximation) that the enthalpy and entropy differences do not depend very much on temperature, leads to

$$\left(\frac{d\Theta}{dT}\right)_{\Theta=0.5} = -\frac{1}{4} \frac{\Delta H}{T^2}. \quad (3)$$

The inverse of Eq. (3) measures the width of the transition (in degrees K). A sharp transition (of a few degrees K) has a high [van't Hoff] ΔH (of the order of 100 Kcal/mol), indicating that perhaps as many as 100 hydrogen bonds are cooperatively broken during the transition.

2.1.2 “Zipper” model family: underlying concepts

Helix *initiation* and helix *growth* are viewed[4] as distinct processes:

- Growth: an existing helix may grow further at the n th site, or shrink. This is viewed as a forward and reverse reaction, with a rate ratio $s = \exp(-\Delta G^*/T)$, which reflects the difference in local free energies between the helix and coil states. If the ratio is greater than unity, the helix has a tendency to grow (“zip”). If it is less than unity, the helix will shrink (“unzip”). At temperatures near the transition, $s \approx 1$. The enthalpy difference $\Delta H^* < 0$ corresponds to the energy of a single hydrogen bond formed in the process of helix growth.
- Nucleation: in order to initiate a helix, 3 residues have to organize themselves. Again, viewing nucleation as a forward / reverse reaction, introduces a dimensionless $\sigma = \exp(-\Delta G_{init}/T)$. The large difference in the free energy comes mostly from the entropy loss associated with the organization of the 3-4 residues involved in the first turn of the helix.

I now present an outline of theoretical models[4], in order of increasing complexity:

2.1.3 “0-th order” - The “all or nothing” (AON) model:

Only two states are significant within this model. The pure coil, with relative statistical weight equal to unity; and the helix with N residues, with a relative weight σs^N . Intermediate states are suppressed, presumably due to high rate barriers. This gives a helix fraction

$$\Theta = \frac{1}{N} \frac{N \sigma s^N}{1 + \sigma s^N} \quad (4)$$

and a slope at midpoint

$$\left(\frac{d\Theta}{dT} \right)_{\Theta=0.5} = \frac{N}{4} \frac{\Delta H^*}{T_m^2}. \quad (5)$$

There is strong cooperativity.

2.1.4 Further considerations: the zipper model

The model allows a single connected helical region of any length $n \leq N$. The statistical weight (Boltzmann factor) is -according to the general considerations, cf. above-, σs^n , and the helix can commence at any of the first $A_n = N - n + 1$ positions. This gives a partition function

$$Z = 1 + \sum_{n=1}^N A_n \sigma s^n \quad (6)$$

and a helical fraction

$$\Theta = \frac{1}{Z} \sum_{n=1}^N n A_n \sigma s^n = \frac{s}{Z} \frac{\partial Z}{\partial s} \quad , \quad (7)$$

where the partition sum can be evaluated to give

$$Z(N) = 1 + \sigma s^{N+2} - (N+1)s + \frac{N}{(s-1)^2} \quad . \quad (8)$$

2.1.5 The generalized zipper model

The only difference is topological; then macromolecule consists of any number of helical and coil regions which may alternate freely. One associates the following weights:

- 1 if coil comes after helix or coil;
- s if helix comes after helix;
- σs if helix comes after coil (nucleation).

The model thus implements the ideas presented in section 2.1.2 without imposing any further constraints. The state of the residue at site i can be described by a 2-vector ν_i , and the partition function is given by

$$\begin{aligned} Z_N &= \sum_{\{\nu_1\} \dots \{\nu_N\}} \langle \nu_1 | T | \nu_2 \rangle \langle \nu_2 | T | \nu_3 \rangle \dots \langle \nu_{N-1} | T | \nu_N \rangle \\ &= \sum_{\{\nu_1\}, \{\nu_N\}} \langle \nu_1 | T^N | \nu_N \rangle \end{aligned} \quad (9)$$

where the matrix elements of \mathbf{T} express the Boltzmann factors specified above, i.e.

$$\mathbf{T} = \begin{pmatrix} s & 1 \\ \sigma s & 1 \end{pmatrix} . \quad (10)$$

To evaluate the partition sum, I apply periodic boundary conditions (convenient, not a must, and certainly wrong for small chains) and obtain

$$Z_N = \text{Tr} \mathbf{T}^N = \lambda_0^N + \lambda_1^N \quad (11)$$

where the eigenvalues are given by

$$\begin{aligned} \lambda_{0,1} &= \frac{1}{2} [1 + s \pm \Delta] \\ \Delta &= \sqrt{(1-s)^2 + 4\sigma s} \end{aligned} \quad (12)$$

and, in the large N limit, Z is dominated by the largest eigenvalue, λ_0 .

Note that the partition function (not the \mathbf{T} -matrix!) can be mapped onto the one of the ferromagnetic Ising model with exchange interaction J and magnetic field h , with the identifications

$$s \Leftrightarrow e^{-2\beta h} \quad (13)$$

$$\sigma \Leftrightarrow e^{-2\beta J} \quad (14)$$

$$\lambda_{\text{magnetic}} = e^{\beta(J+h)} \lambda_{\text{helix-coil}}. \quad (15)$$

To obtain the helix fraction, note that if the probability of obtaining a helical segment of length k is given by $\phi_k(\sigma) k s^k$, where ϕ is the coefficient of s^k in the partition sum. This gives

$$\Theta = \frac{1}{N} \frac{1}{Z} \sum_{k=1}^N \phi_k(\sigma) k s^k = \frac{1}{N} \frac{s}{Z} \frac{\partial Z}{\partial s} \quad (16)$$

One can now verify that as $s \rightarrow 1$, $\Delta \rightarrow 2\sqrt{\sigma}$, $\Theta \rightarrow 1/2$; for $\sigma \ll 1$ (cf. below),

$$\left(\frac{d\Theta}{dT} \right)_{\Theta=0.5} = \frac{1}{4\sqrt{\sigma}} \frac{\Delta H^*}{T_m^2}. \quad (17)$$

The experimental situation[3] for long ($N = 1500$) chains is summarized in Fig. 1. Fits can be obtained with $\Delta H^* = -3.8 \text{ kJ/mole}$ (cf. calorimetric measurements $\Delta H = -3.97 \text{ kJ/mole}$) and $\sigma = 1.6 \times 10^{-4}$. One usually interprets $1/\sqrt{\sigma}$ as number of residues cooperatively involved in the transition (cf. AON theory, Eq. 5). This interpretation also follows from the Ising model, where the inverse correlation length is given (in lattice constants) by

$$1/\xi = \lambda_1 - \lambda_0 = 2\sqrt{\sigma} \quad (\text{at } s = 1). \quad (18)$$

The following simple conformational argument provides an independent estimate for $\sigma = e^{-\Delta G_{\text{init}}/T} \approx e^{\Delta S_{\text{init}}}$. Initiation of the helix involves organization of J ($=3$ or 4) residues, each one by 2 dihedral angles. Typically a dihedral angle can take 3 independent orientations in space. This gives a total of 3^{2J} states, or an entropy loss $\Delta S_{\text{init}} = -2J \ln 3$. ($=-6.6$ for $J = 3$, or -8.8 for $J = 4$). This compares favorably with $\ln(2 \times 10^{-4}) = -8.5$.

Similarly, one can relate the entropy loss involved in helix *growth*, to the energy of the H-bond. At the transition, $\Delta S^* = \Delta H^*/T_m = -1.85$. This is roughly comparable to the estimate $-2 \ln 3 \approx -2.20$, obtained by considering the 2 dihedral angles which must be organized to admit a residue into the helix.

2.1.6 A useful shortcut

It is possible to obtain the thermodynamics of the generalized zipper model without recourse to the transfer matrix formalism. I present this “hand-waving” [5], because it will be useful for DNA loops (cf. below).

The fundamental “entity” of the macromolecule is a helical region of length n , followed by a coil region of length m . This “helix-coil” entity is characterized by a free energy

$$g(n, m) = -T \ln \sigma - nT \ln s \quad (19)$$

where the two terms correspond to the contributions of helix nucleation and growth, respectively; it occurs with a probability

$$P_{n,m} = \exp\{-[g(n, m) - g_0]/T\} \quad (20)$$

where $g_0 \equiv -T \ln z$ is the equilibrium free energy per site of the full macromolecule, to be determined by the normalization condition

$$\sum_{n,m=1}^{\infty} P_{n,m} = 1 \quad . \quad (21)$$

Both the n and the m - summations can be done trivially as long as $s < z$ and $z > 1$. The condition (21) can then be written as

$$\frac{s}{z-s} \frac{1}{z-s} = \frac{1}{\sigma} \quad , \quad (22)$$

whose roots are identical to those of (13) obtained via the transfer matrix; the largest root is the one which satisfies the condition $z > \max(1, s)$ (cf. above).

2.2 Loop entropies and DNA denaturation

2.2.1 Background

Thermal DNA denaturation occurs when the two strands of the double helix separate upon heating. In real DNA the phenomenon of multistep melting is ubiquitous, reflecting the inhomogeneity of the molecule. “Homogeneous”, synthetic DNA, which consists of a few thousand identical base pairs has been studied experimentally[6] and shown to exhibit a very sharp transition; the qualitative shape of the coil fraction curve, as obtained by optical density or viscosity measurements, is similar to that of Fig. 1; however, the observed temperature width is of the order of one degree. It is reasonable to speculate that in the thermodynamic limit the transition would be of the first order. Poland and Scheraga[7](PS) proposed a simple model of the thermodynamics involved, based on the ideas discussed in Section 2.1.2, and the concept of loop entropy (cf. below). There is however a difference in the physical origin of the parameters involved; the helix growth probability $s = \exp\{-\epsilon/T\}$ now reflects the combined effect of both interactions which are significant in the bonded DNA state: the hydrogen bonding responsible for binding base pairs and the stacking interaction between adjacent bases.

2.2.2 Loop entropies

A denaturation loop of length m , i.e. a region of m sites where the double helix has locally melted, is characterized by the extra entropy it contributes[7]. This extra entropy has been calculated for lattice polymers and is of the form

$$S_L(m) = am + b - c \ln m \quad , \quad (23)$$

where a and b are constants and c depends on the dimensionality. In the case of Gaussian polymer chains, or random lattice walks, which ignore the effects of excluded volume, $c = d/2$. Taking account of excluded volume tends to increase the value of c . It will be seen below that this can have a decisive influence on the nature of the transition.

2.2.3 The phase transition

In an infinitely long DNA molecule, the fundamental entity is again a double-helical region of n sites (base pairs), followed by a denaturation loop of length m ($2m$ bases); putting together the contributions from helical and loop part (cf. Sections 2.2.1 and 2.2.2), I obtain the free energy of this entity as

$$g(n, m) = -T \ln \sigma + n\epsilon - mT \ln u^2 + Tc \ln m \quad (24)$$

where $u = \exp(a/2)$ is another constant, and I have dropped the irrelevant constant b . It is now possible to derive the thermodynamics exactly as in section 2.1.6. Inserting (24) in the normalization condition (21) gives

$$\frac{z}{s} - 1 = \sigma U \left(\frac{z}{u^2} \right) \quad , \quad (25)$$

where $s = \exp(-\epsilon/T)$ is the only temperature dependent parameter, and

$$U(x) = \sum_{m=1}^{\infty} \frac{1}{m^c} \left(\frac{1}{x} \right)^m \quad . \quad (26)$$

Near $x = 1$ it is possible to approximate $U(x)$ by the expression[8]

$$U(x) \approx U_0 - U_1 \left[1 - \frac{1}{x} \right]^{c-1} \quad (27)$$

where, for $c > 1$, $U_0 \approx U_1 \approx \zeta(c)$ [1].

I now follow the thermodynamic behavior near the putative singularity by defining[8] an $s_c \equiv \exp(-\epsilon/T_c)$ via

$$\frac{u^2}{s_c} - 1 = \sigma U(1) \quad (28)$$

and subtracting (28) from (25) to obtain

$$s_c - s + \Delta + \frac{\sigma s_c}{u^2} U_1 \Delta^{c-1} = 0 \quad , \quad (29)$$

where $z = u^2(1 + \Delta)$ and I have only kept lowest order terms in the small quantities Δ and $s - s_c$. It is now straightforward to use (29) and obtain $\Delta(s)$; the helix fraction is then given by

$$\frac{\partial \ln z}{\partial \ln s} \propto \frac{\partial \Delta}{\partial s} \quad . \quad (30)$$

Two cases can be distinguished:

- $1 < c < 2$. The linear term in Δ can be neglected in (29). The helix fraction is proportional to $(T_c - T)^{(2-c)/(c-1)}$, i.e. it approaches zero continuously near the transition. In particular, if $c = 3/2$ (the value which corresponds to $d = 3$ and neglecting excluded volume effects), one obtains a second order transition.
- $c > 2$. The linear term in Δ dominates, and the transition becomes first order, i.e. the helix fraction drops abruptly to zero at the transition.

The above analysis shows how crucial the value of c is in determining the nature of the transition. It has been long known[8] that excluded volume effects, as calculated within the framework of self-avoiding walks, can increase the value of c to 1.75 for loops embedded in three-dimensional space. Recent research[9] suggests that c may be as high as 2.1.

3 Hamiltonian approach to DNA denaturation

3.1 The model

A “minimal” Hamiltonian model of homogeneous DNA denaturation has been proposed by Peyrard and Bishop[10](PB). The model assumes two parallel, harmonic chains, with lattice constant l , joined in the form of a ladder by anharmonic springs; the particular model proposes a Morse potential because of its analytical tractability, although any form with a repulsive core, a stable minimum and a flat top (e.g. Lennard-Jones) would be physically suitable. The emphasis is on modelling the unbinding of the two chains, not the helical aspect of the ordered state; this is done in the general spirit of the theory of critical phenomena, which has demonstrated that the “essentials” of the interactions completely determine the critical

behavior. The Hamiltonian

$$\begin{aligned}
H_{tot} &= \frac{m}{2} \sum_n \left[\dot{u}_n^2 + \dot{v}_n^2 + \omega_0^2 (u_n - u_{n-1})^2 + \omega_0^2 (v_n - v_{n-1})^2 \right] \\
&+ \sum_n V(u_n - v_n)
\end{aligned} \tag{31}$$

describes the motion of the two bound chains with coordinates $\{u_n\}, \{v_n\}$; dots denote time derivatives; only the motion transverse to the chains is considered; bases have equal masses m and are connected by harmonic springs of equal strength, determined by the frequency ω_0 ; the energy scale of the Morse potential

$$V(x) = D(e^{-ax} - 1)^2 \tag{32}$$

is given by D and its spatial range by $1/a$.

Transformation to center-of-mass and relative coordinates, $Y_n = (u_n + v_n)/2, y_n = u_n - v_n, M = 2m, 1/\mu = 2/m$ decouples center-of-mass from relative motion, i.e.

$$H_{tot} = H_0(Y) + H(y) \quad , \tag{33}$$

where

$$H_0(Y) = \sum_n \left[\frac{P_n^2}{2M} + \frac{1}{2} M \omega_0^2 (Y_n - Y_{n-1})^2 \right] \quad , \tag{34}$$

$P_n = M \dot{Y}_n$ is the canonical momentum conjugate to Y_n , and

$$H(y) = \sum_n \left[\frac{p_n^2}{2\mu} + \frac{1}{2} \mu \omega_0^2 (y_n - y_{n-1})^2 + V(y_n) \right] \quad , \tag{35}$$

where $p_n = \mu \dot{y}_n$ is the canonical momentum conjugate to y_n .

3.2 Statistical Mechanics

H_0 is just the Hamiltonian of a harmonic chain with the total base pair mass $2m$ per site. It gives an additive nonsingular contribution to all thermal properties. It will be neglected in what follows. The classical thermodynamics of H is described by the canonical partition function

$$Z = \int \prod_{n=1}^N dp_n dy_n e^{-\beta H} \quad . \tag{36}$$

One can immediately perform the Gaussian integrals over momentum space and obtain

$$Z = Z_K Z_P, \tag{37}$$

where each integration in the kinetic part contributes a $(2\pi\mu/\beta)^{1/2}$ factor to the partition function, i.e.

$$Z_K = (2\pi\mu/\beta)^{N/2} \quad . \quad (38)$$

The nontrivial part is

$$Z_P = \int \left(\prod_{n=1}^N dy_n \right) T(y_1, y_2) \cdots T(y_{N-1}, y_N) T(y_N, y_{N+1}) \quad , \quad (39)$$

where

$$T(x, y) = e^{-\beta \left[\frac{\mu\omega_0^2}{2}(y-x)^2 + V(x) \right]} \quad . \quad (40)$$

3.3 Transfer integral: the formalism

3.3.1 Definitions and Notation

Consider the eigenvalue problem defined by the asymmetric kernel T (the kernel can be easily symmetrized but need not be so; in fact, working with the asymmetric kernel is technically advantageous in examining the validity of some approximations, cf. below):

$$\int_{-\infty}^{\infty} dy T(x, y) \Phi_{\nu}^R(y) = \Lambda_{\nu} \Phi_{\nu}^R(x) \quad (41)$$

$$\int_{-\infty}^{\infty} dy T(y, x) \Phi_{\nu}^L(y) = \Lambda_{\nu} \Phi_{\nu}^L(x) \quad , \quad (42)$$

where left and right eigenstates have been assumed to be normalized; note that the normalization integral is $\int dx \Phi_{\nu}^L(x) \Phi_{\nu}^R(x)$. Orthogonality

$$\int_{-\infty}^{\infty} dx \Phi_{\nu}^L(x) \Phi_{\nu'}^R(x) = \delta_{\nu\nu'} \quad (43)$$

and completeness

$$\sum_{\nu} \Phi_{\nu}^L(x) \Phi_{\nu}^R(y) = \delta(x - y) \quad (44)$$

relationships are assumed to hold. Note that this is not obvious for the class of potentials of interest here. This is a point which will be further taken in section 3.6. I will further use the notation

$$\Lambda_{\nu} = e^{-\beta\epsilon_{\nu}} \quad (45)$$

(sensible as long as the eigenvalues are nonnegative).

3.3.2 The partition function

The integrand of (39), as written down has a problem: it includes a reference to the displacement y_{N+1} of the $N + 1$ st particle, which has not yet been defined. For a large system, this is best remedied by means of periodic boundary conditions (PBC), i.e. by demanding that $y_{N+1} = y_1$. Alternatively, the integration may be extended to one more variable, dy_{N+1} , with the simultaneous introduction of a factor $\delta(y_{N+1} - y_1)$ to take care of PBC. This however is the same as the sum in the left-hand-side of (44). I then obtain

$$Z_P = \sum_{\nu} \int dy_1 \cdots \underbrace{dy_{N+1} \Phi_{\nu}^L(y_1)}_{\text{}} T(y_1, y_2) \cdots \underbrace{T(y_N, y_{N+1}) \Phi_{\nu}^R(y_{N+1})}_{\text{}} . \quad (46)$$

The braces make clear that I can perform the integral over dy_{N+1} and obtain a factor $\Lambda_{\nu} \Phi_{\nu}^R(y_{N+1})$, using the defining property of right-hand eigenfunctions. The process can be repeated N times, each time giving a further factor Λ_{ν} and a right eigenfunction with an argument whose index is smaller by one. At the end, I am left with

$$Z_P = \sum_{\nu} \int dy_1 \Phi_{\nu}^L(y_1) \Lambda_{\nu}^N \Phi_{\nu}^R(y_1) = \sum_{\nu} \Lambda_{\nu}^N . \quad (47)$$

In the thermodynamic limit, Z_P is dominated by the largest eigenvalue Λ_0 or, equivalently, the lowest ϵ_0 :

$$\lim_{N \rightarrow \infty} \frac{1}{N} \ln Z_P = \ln \Lambda_0 = -\beta \epsilon_0 \quad (48)$$

3.3.3 The order parameter

$$\begin{aligned} \langle y_i \rangle &= \frac{1}{Z_P} \int dy_1 \cdots dy_N T(y_1, y_2) \cdots T(y_{i-1}, y_i) y_i \\ &\quad T(y_i, y_{i+1}) \cdots T(y_N, y_{N+1}) \\ &\equiv \frac{1}{Z_P} \sum_{\nu} \int dy_1 \cdots dy_{N+1} \Phi_{\nu}^L(y_1) \underbrace{T(y_1, y_2) \cdots T(y_{i-1}, y_i)}_{i-1} y_i \\ &\quad \underbrace{T(y_i, y_{i+1}) \cdots T(y_N, y_{N+1})}_{N-i+1} \Phi_{\nu}^R(y_{N+1}) , \end{aligned} \quad (49)$$

after insertion of a complete set of states (cf. above); the braces denote the number of times I can perform an integration and obtain, respectively, a right eigenfunction with an argument smaller by one, or a left eigenfunction with an argument larger by one, as well as a factor Λ_{ν} . The remaining

integral must be performed explicitly:

$$\begin{aligned} \langle y_i \rangle &= \frac{1}{Z_P} \sum_{\nu} \Lambda_{\nu}^N M_{\nu\nu} \\ &\approx M_{00} \end{aligned} \quad (50)$$

where the second line is exact in the thermodynamic limit, and I have used the abbreviation

$$M_{\nu\mu} = \int_{-\infty}^{\infty} dy \Phi_{\nu}^L(y) y \Phi_{\mu}^R(y) \quad . \quad (51)$$

3.3.4 Correlations

With $i < j$,

$$\begin{aligned} \langle y_i y_j \rangle &\equiv \frac{1}{Z_P} \int dy_1 \cdots dy_N T(y_1, y_2) \cdots T(y_{i-1}, y_i) y_i T(y_i, y_{i+1}) \\ &\quad \cdots T(y_{j-1}, y_j) y_j T(y_j, y_{j+1}) \cdots T(y_N, y_{N+1}) \\ &= \frac{1}{Z_P} \sum_{\nu} \int dy_i \cdots dy_j \Lambda_{\nu}^{i-1} \Phi_{\nu}^L(y_i) y_i T(y_i, y_{i+1}) \\ &\quad \cdots T(y_{j-1}, y_j) y_j \Lambda_{\nu}^{N-j+1} \Phi_{\nu}^R(y_j) \end{aligned} \quad (52)$$

where the straightforward integrations, i.e the first $i-1$ and the last $N-j+1$ have already been performed (cf. above). In order to perform the remaining integrations, I insert two more factors of 1, after y_i and before y_j , i.e. integrals $\int \delta(y_i - \bar{y}_i)$ and $\int \delta(y_j - \bar{y}_j)$, respectively; exploiting the presence of the δ functions, I may substitute the variables y_i and y_j by \bar{y}_i and \bar{y}_j respectively. This translates to two more sums over complete sets of states and another $j-i$ integrals which can now be performed:

$$\begin{aligned} \langle y_i y_j \rangle &= \frac{1}{Z_P} \sum_{\nu, \mu, \rho} \int d\bar{y}_i d\bar{y}_j dy_i \cdots dy_j \Lambda_{\nu}^{i-1} \Phi_{\nu}^L(\bar{y}_i) \bar{y}_i \Phi_{\mu}^R(\bar{y}_i) \Phi_{\mu}^L(y_i) \\ &\quad T(y_i, y_{i+1}) \cdots T(y_{j-1}, y_j) \Phi_{\rho}^R(y_j) \Phi_{\rho}^L(\bar{y}_j) \bar{y}_j \Lambda_{\nu}^{N-j+1} \Phi_{\nu}^R(\bar{y}_j) \\ &= \frac{1}{Z_P} \sum_{\nu, \mu, \rho} \Lambda_{\nu}^{N+i-j} \Lambda_{\rho}^{j-i} \int d\bar{y}_i d\bar{y}_j \Phi_{\nu}^L(\bar{y}_i) \bar{y}_i \Phi_{\mu}^R(\bar{y}_i) \\ &\quad \delta_{\mu, \rho} \Phi_{\rho}^L(\bar{y}_j) \bar{y}_j \Phi_{\nu}^R(\bar{y}_j) \\ &= \frac{1}{Z_P} \sum_{\nu, \mu} \Lambda_{\nu}^{N+i-j} \Lambda_{\mu}^{j-i} |M_{\nu\mu}|^2 \quad . \end{aligned} \quad (53)$$

In the thermodynamic limit the $\nu = 0$ term dominates; the resulting factor cancels against the denominator and leaves

$$\langle y_i y_{i+r} \rangle = \sum_{\mu} |M_{0\mu}|^2 e^{-\beta(\epsilon_{\mu} - \epsilon_0)r} \quad (54)$$

where I have used Dirac shorthand for the matrix element and set $j = i + r$. The first term ($\mu = 0$) in the above sum corresponds to $\langle y \rangle^2$ and should properly be subtracted from both sides; This leaves

$$\begin{aligned} \langle \delta y_i \delta y_{i+r} \rangle &\equiv \langle y_i y_{i+r} \rangle - \langle y_i \rangle \langle y_{i+r} \rangle \\ &= \sum_{\nu}' |M_{0\nu}|^2 e^{-\beta(\epsilon_\nu - \epsilon_0)r} \end{aligned} \quad (55)$$

where now the ground state is excluded from the summation. The above result identifies the correlation length ξ , i.e the typical length over which the decay of correlations takes place, as

$$\frac{\xi}{l} = \frac{1}{\beta(\epsilon_1 - \epsilon_0)} \quad (56)$$

where the subscript 1 stands for the first excited state (dominant exponential in the limit of large r).

3.4 TI results: Gradient-expansion approximation

Suppose that the displacement field does not change appreciably over a lattice constant. This is certainly reasonable at low temperatures. Note that this does not exclude large displacements per se. Nonlinearity is explicitly allowed, but the displacement field must be smooth. The assumption is certainly reasonable at low temperatures.

I set $y = x + z$, $\Phi^R \rightarrow \phi$ and rewrite (41) as

$$\begin{aligned} e^{-\beta[\epsilon_\nu - V(x)]} \phi_\nu(x) &= \int_{-\infty}^{+\infty} dz e^{-\frac{1}{2}\beta\mu\omega_0^2 z^2} \left\{ \phi_\nu(x) + z\phi'_\nu(x) + \frac{1}{2}z^2\phi''_\nu(x) \right\} \\ &= \left[\frac{2\pi}{\beta\mu\omega_0^2} \right]^{1/2} \left\{ \phi_\nu(x) + \frac{1}{2\beta\mu\omega_0^2} \phi''_\nu(x) \right\} \end{aligned} \quad (57)$$

where higher terms in the gradient expansion have been neglected and the Gaussian integrals have been performed; this is meaningful as long as the width of the Gaussians is smaller than the range of the Morse potential, i.e.

$$\beta\mu\omega_0^2/a^2 > 1 \quad . \quad (58)$$

The factor in front of the r.h.s. of (57) can be absorbed in the eigenvalue by defining $\tilde{\epsilon}_\nu = \epsilon_\nu + 1/(2\beta) \ln[2\pi/(\beta\mu\omega_0^2)]$. Now, for many practical purposes, when it comes to calculating matrix elements, the relevant magnitude of $\epsilon - V(x)$ is D , the depth of the Morse well (or some other characteristic energy in the case of another potential). The key to this statement is that one does not need to consider large negative values of x , where $V(x)$ is huge, because at such x , both the exact eigenfunction Φ and its approximation

ϕ can be expected to be negligible. If then $\beta D \leq 1$ ¹ it is reasonable to expand the exponential and keep only the first term. Dividing both sides by β , I obtain a Schrödinger - like equation,

$$-\frac{1}{2\mu(\beta\omega_0)^2}\phi''_\nu(x) + [V(x) - \tilde{\epsilon}_\nu]\phi_\nu(x) = 0 \quad . \quad (59)$$

Before continuing the discussion of (59) and its properties, I pick up the bits and pieces (cf (37), (38), (48)) of the thermodynamic free energy (per site)

$$f = -\frac{1}{\beta N} \ln(Z_K Z_P) \equiv -\frac{1}{\beta} \ln \left(\frac{2\pi}{\beta\omega_0} \right) + \tilde{f} \quad , \quad (60)$$

where $\tilde{f} = \tilde{\epsilon}_0$. The first term in (60) is the free energy of the small oscillations (transverse phonons in this context). It is a term smooth in temperature (constant specific heat!) and therefore irrelevant to any phase transition. Any nontrivial physics is hidden in the second term, which is identical with the the smallest eigenvalue of (59).

A couple of comments are in order. First, (59) would be a literal (i.e. quantum-mechanical) Schrödinger equation, if I substituted $1/(\beta\omega_0)$ by \hbar . I will come back to that point. Second, I can get a dimensionless potential (and eigenvalue) by dividing both sides of (59) by D . In other words, the relevant dimensionless parameter is

$$\delta^2 = \begin{cases} \frac{2\mu}{a^2\hbar^2} \cdot D & \text{(quantum mechanics)} \\ \frac{2\mu\beta^2\omega_0^2}{a^2} \cdot D & \text{(statistical mechanics).} \end{cases} \quad (61)$$

In terms of δ , the bound state spectrum of (59) is given [11] by

$$\begin{aligned} \frac{\tilde{\epsilon}_n}{D} &= 1 - \left[1 - \frac{n+1/2}{\delta} \right]^2 \\ n &= 0, 1, \dots, \text{int}(\delta - 1/2) . \end{aligned} \quad (62)$$

There is at least one bound state if $\delta > 1/2$. For $1 \geq \delta > 1/2$ there is *exactly* one bound state. And if δ becomes equal to, or smaller than $1/2$, there is no bound state at all. *The value $\delta_c = 1/2$ is "critical"*. In quantum mechanical language, if a particle has a mass which is lighter than a critical mass $\mu_c = \hbar^2 a^2 / (8D)$, it cannot be confined in the Morse well. Quantum fluctuations will drive it out². In the context of statistical mechanics, δ_c

¹Note that, in connection with (58), this defines a temperature window $D < k_B T < \mu\omega_0^2/a^2$ for the validity of the overall approximation scheme.

²This is a general property of asymmetric one-dimensional wells; symmetric wells will support a particle in a bound state, no matter how low its mass.

corresponds, via (61), to a critical temperature $T_c = 2(\omega_0/a)\sqrt{2\mu D}$. The free energy is given by

$$\frac{\tilde{f}}{D} = \begin{cases} 1 & T > T_c \\ 1 - \left(1 - \frac{T}{T_c}\right)^2 & T < T_c \end{cases}, \quad (63)$$

where in the upper line I have made use of the fact that the bottom of the continuum part of the spectrum is at $\epsilon = D$. The free energy f is non-analytic at $T = T_c$, where its second derivative is discontinuous (i.e. there is a jump in the specific heat). This corresponds to a second order transition, according to the Ehrenfest classification scheme³.

In order to gain some further insight into the physics involved⁴ it is useful to examine the average displacement (50), determined by the ground-state (GS) eigenfunction

$$\phi_0(x) = e^{-\zeta/2} \zeta^{\delta-1/2} \quad (64)$$

where $\zeta = 2\delta e^{-ax}$. It is straightforward to see that, as T approaches T_c from below, the eigenfunction extends towards larger and larger positive values of x :

$$\phi_0(x) \propto e^{-\lambda x} \quad (65)$$

where

$$\lambda = \frac{1}{\delta - \delta_c} \quad (66)$$

is a (transverse) characteristic length which measures the spatial extent of the GS eigenfunction. As a consequence, we can estimate that $\langle y \rangle$, which is dominated by the large values of the argument, will also behave as

$$\langle y \rangle \sim (\delta - \delta_c)^{-1} \sim \left(1 - \frac{T}{T_c}\right)^{-1}. \quad (67)$$

As the critical temperature is approached from below, particles cease to be confined to the minimum of the Morse well. They perform larger and larger excursions to the flatter part of the potential. At T_c the transition is

³Note that the term "second order" is meant literally in this case, not just as a metaphor for the absence of a latent heat (for which the term "continuous transition" would be appropriate).

⁴The mathematical analogy between the behavior of the spectral gap which occurs in a point ($d = 0$) system and the singularity in the free energy of a classical chain ($d = 1$) is an example of a deeper analogy which relates quantum to thermal fluctuations; the formal correspondence $\hbar \leftrightarrow 1/(\beta\omega_0)$ manifests a far-reaching analogy between d -dimensional quantum mechanics and $(d+1)$ -dimensional classical statistical mechanics. The analogy is most fruitful at $d = 1$, because of the interplay and the richness of exact available results which based either in the transfer-matrix approach of 2-dimensional classical statistics or on the Bethe-Ansatz developed for 1-d quantum spin systems.

complete; the average transverse displacement is infinite. Particles move, on the average, on the flat top of the Morse potential. Unwinding (“melting”) of the DNA has occurred.

In the language of critical phenomena $\langle y \rangle$ is the order parameter. In the “usual” phase transitions, one goes from an ordered to a disordered phase. The order parameter m vanishes at the transition point, i.e. $m \propto (T_c - T)^\beta$ with a positive critical exponent β (not to be confused with the inverse temperature: standard notation of critical phenomena!). DNA melting is really an instability[12] - rather than an “order-disorder” transition. It is therefore not surprising that the corresponding critical exponent β extracted from (67) is negative (-1).

Experimental data on DNA denaturation do not deliver $\langle y \rangle$ directly. The “experimental order parameter” is the helical fraction, i.e. the probability that a given base pair is still bound; technically one uses an (instrumentation-dependent) cutoff y_0 and measures $P(y > y_0, T)$. For the model presented here, this function approaches zero smoothly (linearly) as $T \rightarrow T_c$, independently of the choice of y_0 .

Eq. (56) states that the correlation length is also controlled by the gap in the eigenvalue spectrum; as the transition is approached,

$$\frac{\xi}{l} = \frac{1}{\beta D} \left(1 - \frac{T}{T_c}\right)^{-2} \quad (68)$$

which identifies a critical exponent $\nu = 2$ for the divergence of the correlation length. The picture of thermal denaturation which emerges is one of ordered regions, where helical structure persists; these regions are interrupted by droplets of the high-temperature phase, i.e. “denaturation bubbles” of typical size ξ .

3.5 A first order transition?

It is possible to generalize the theory in order to take account of the fact that the stacking energy is a property of successive base pairs, rather than individual bases. A practical way of doing this is to substitute the second term in the Hamiltonian (35) by

$$\frac{1}{2} \mu \omega_0^2 [1 + g(y_n + y_{n-1})] (y_n - y_{n-1})^2 \quad , \quad (69)$$

where [13]

$$g(x) = e^{-\alpha x} \quad . \quad (70)$$

The effect of Eqs. (69)-(70) is to interpolate between the original value of the elastic coupling if *either* (or both) of the two base pairs n , $n - 1$ is unbound (in which case $y_n \rightarrow \infty$ or $y_{n-1} \rightarrow \infty$), and twice that value if both are bound; in the latter case, typically, $y_n \approx 0$; the much higher

values of the stacking energy, which (70) in principle allows, are statistically irrelevant due to the repulsive core of the Morse potential. Within the gradient expansion approximation, it can be shown[15] that the main effect of the nonlinear stacking energy on the thermodynamics is to generate an effective, on-site, “thermally activated” barrier

$$U(y) = \frac{T}{2D} \ln(1 + e^{-2\alpha y}) \quad . \quad (71)$$

which appears in Eq. 59 and acts in addition to the Morse potential.

It has been shown[14, 15, 17] that the character of the transition changes dramatically as the value of the stacking parameter ratio α/a decreases (corresponding to a longer range in the effective potential). Although the transition remains asymptotically second order, the limiting asymptotic behavior becomes relevant only within an exponentially small range of the temperature difference $T_c - T$. For all practical purposes, the transition is first order, with a finite melting entropy $\Delta S = A_0 D/T_c$, where A_0 is a numerical constant of order unity[15].

It should be noted that the interpolation (70) is not unique; an interpolation function of the type $g(x) = 1, x < x_0, g(x) = (x_0/x)^2, x > x_0$, leads - depending on the other parameters - to a rich variety of critical behavior, ranging from a first-order transition to continuously varying critical exponents.[16]

With the above modification (69), it has become possible[17] to describe, at least in principle, the series of multistep melting observed in real, heterogeneous DNA.

3.6 TI beyond the gradient expansion

It was stated in Section 3.3.1 that the TI formalism rests on the assumption that the integral equations (41) and (42) - have a complete, orthonormal set of eigenfunctions. Within the gradient approximation approach this was demonstrated by construction - since the integral equation was reduced to a Schrödinger-like equation. In many cases however, the gradient expansion is not valid at all. It is therefore necessary to develop alternative, mostly numerical methods for computing TI thermodynamics. For such applications it is expedient to consider the symmetrized, dimensionless version of the kernel (40), i.e.

$$T_s(x, y) = e^{-[(y-x)^2/R + V(x) + V(y)]/(2T)} \quad (72)$$

and the associated integral equation

$$\int_{-\infty}^{\infty} dy T_s(x, y) \phi(y) = \Lambda \phi(x) \quad , \quad (73)$$

where $R = Da^2/(\mu\omega_0^2)$, $T = 1/(\beta D)$ and the Morse potential is now dimensionless, $V(x) = (1 - e^{-x})^2$, as are the displacement variables x, y .

Due to the flat top of the Morse potential, the kernel (72) is not of the Hilbert-Schmidt type[18]; therefore the integral equation (73) is singular and it can not be a priori stated that it possesses a complete orthonormal set of eigenstates; in other words, the prerequisites for directly applying the TI method are not strictly met. In the rest of this section I will outline a mathematically consistent procedure of examining the spectral gap of (73), based on finite-size scaling concepts[19].

Due to the presence of the Gaussian factors in the kernel, it is possible to approximate the integral in the left-hand-side of (73) by using a Gauss-Hermite grid of size N , i.e.

$$\int_{-\infty}^{\infty} d\bar{y} e^{-\bar{y}^2} f(\bar{y}) \approx \sum_{m=1}^N w_m f(\bar{y}_m) \quad (74)$$

where the positions $\{\bar{y}_m\}$ and weights $\{w_m\}$ are given by the appropriate Gauss-Hermite quadratures routine. The largest $\bar{y}_N \approx (2N + 1)^{1/2} \equiv L$ can be used as estimate of the *transverse* “size of the system” employed at any given discretization. I emphasize transverse because the length of the chain is infinite, i.e. the thermodynamic limit has already been taken.

I use “rescaled” variables, i.e. $y = \rho\bar{y}$, $\rho = (2RT)^{1/2}$, divide both sides of (73) by $\rho\sqrt{\pi}$, and use the approximation (74). The result is an approximation of (73) by the matrix eigenvalue equation

$$\sum_{j=1}^N D_{ij} A_j^\nu = \tilde{\Lambda}_\nu A_i^\nu \quad (75)$$

where

$$D_{ij} = \left(\frac{w_i w_j}{\pi}\right)^{1/2} e^{\bar{y}^i \bar{y}^j} e^{-(\bar{y}^i - \bar{y}^j)^2/2} e^{-[V(\rho\bar{y}^i) + V(\rho\bar{y}^j)]/(2T)} \quad (76)$$

and $\tilde{\Lambda}_\nu \equiv \Lambda_\nu/(2\pi RT)^{1/2} \equiv e^{-\epsilon_\nu/T}$.

It is now possible to solve numerically the real, symmetric matrix eigenvalue problem (76) for a range of temperatures and a sequence of increasingly fine grids. Results for the difference between the two lowest eigenvalues are shown in Fig. 2 for $R = 10.1$. For any given size L , the gap has a minimum $\Delta\epsilon_m(L)$ at a certain temperature $T_m(L)$. Fig. 3 demonstrates that (i) the value of the gap approaches zero quadratically as $L \rightarrow \infty$ (with an accuracy of 10^{-5}), and (ii) the sequence of $T_m(L)$ ’s also approaches a limiting value $T_c = 1.2275$ quadratically.

It is natural to identify the limiting temperature T_c , where the spectral gap of the limiting, infinite-dimensional matrix eigenvalue equation (75) vanishes, as the transition temperature of the original TI equation (73).

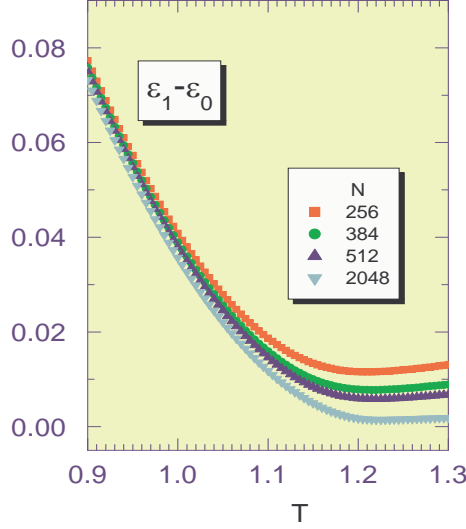


Figure 2: The gap between the two lowest eigenvalues of the matrix eigenvalue problem (75), for a variety of N values. For a given N , the gap has a minimum at a certain temperature T_m .

Further application of finite-size scaling methods demonstrates[19] that the various critical exponents coincide with those obtained within the gradient expansion method.

Acknowledgments

I thank M. Peyrard and T. Dauxois for many helpful discussions and comments.

Appendix: Phase transitions in one-dimensional systems

I briefly discuss why the general prohibitions on phase transitions in one dimension are inapplicable to both the PS and the PB models of DNA denaturation.

Van Hove's theorem[21] states that no phase transitions occur in 1-d particle systems with short-range pair interactions. The PB model has on-

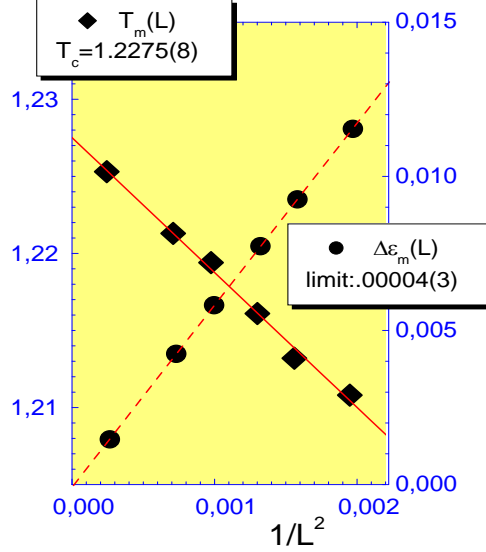


Figure 3: The magnitude of the gap minimum (circles, right y-axis scale) approaches zero as the system size goes to infinity. The sequence of the temperatures corresponding to the gap minima, $T_m(L)$ (diamonds, left y-axis scale), can be used to provide an estimate of the critical point T_c .

site potential - i.e. the theorem is not applicable. It is however worth noting that similar mathematical proofs, have been given for systems with periodic on-site potentials[22]. Such proofs however seek to prove analyticity of the eigenvalue spectrum and hence absence of a phase transition; as such, they tend to exclude potentials which give rise to singular TI equations.

The PS model is not a Hamiltonian model and therefore van Hove's theorem is again not applicable.

Landau's theorem[23] is significantly stronger. It states that “macroscopic phase coexistence cannot occur at finite temperatures in one dimensional systems”. It is less obvious why it should not apply. I therefore outline the proof. Consider a system with N sites, which may exist in either phase A or phase B . Let θ be the fraction of phase A ; furthermore, let there be $m \ll N$ contacts between the phases, each of energy ϵ . These can be steplike (Ising) or continuous domain walls. The free energy of the configuration is given by

$$F = N\theta f_A + N(1 - \theta)f_B + F_{DW} \quad (\text{A.77})$$

where

$$F_{DW} = m\epsilon - k_B T S_{DW}(m, N) \quad (\text{A.78})$$

and the (dimensionless) entropy is given by

$$S_{DW}(m, N) = \ln \left[\frac{N!}{m!(N-m)!} \right] \approx m \ln \left[\frac{Ne}{m} \right] \quad (\text{A.79})$$

Minimization of the total free energy with respect to m yields a macroscopic average number (ie. a *finite density*) of domain walls

$$\bar{m} = Ne^{-\epsilon/(k_B T)} \quad (\text{A.80})$$

The system breaks up into m regions of finite size $e^{\epsilon/(k_B T)}$. Macroscopic phase separation can only occur at zero temperature (as the domain size goes to infinity).

Landau's argument covers a wide range of systems, e.g. double-well on-site potentials (Ising universality class), or periodic on-site potentials. It does not cover the PB case, because the DW has infinite energy[20]. It does not apply to the PS case because the loop entropy is not proportional to the size of the loop and therefore (A.77) does not hold. On the contrary, the theorem is applicable to the generalized zipper model, as its authors had correctly noted[4].

References

- [1] A definitive review of the subject has been given by D. Poland and H. A. Scheraga, *Theory of helix-coil transitions in biopolymers*, Academic (1970).
- [2] e.g. T.E. Creighton, *Proteins*, W.H. Freeman (1992).
- [3] B.H. Zimm, P. Doty and K. Iso, *Proc. Nat. Acad. Sc. (USA)*, **45**, 1601 (1959); V.A. Bloomfield, *Am. J. Phys.* **67**, 1212 (1999).
- [4] B.H. Zimm and J.R. Bragg, *J. Chem. Phys.* **31**, 526 (1959).
- [5] M. Ya. Azbel, *Phys. Rev.* **A10**, 1671 (1979).
- [6] (a) A. Wada, S. Yabuki and Y. Husimi, *CRC Crit. Rev. Biochem.* **9**, 87 (1980); (b) J. de Ley, *J. Theor. Biol.* **22**, 89 (1969); (c) R.B. Inman and R.L. Baldwin, *J. Mol. Biol.* **8**, 452 (1964).
- [7] D. Poland and H. A. Scheraga, *J. Chem. Phys.* **45**, 1464 (1966).
- [8] M.E. Fisher, *J. Chem. Phys.* **45**, 1469 (1966).
- [9] Y. Kafri, D. Mukamel and L. Peliti, *Phys. Rev. Lett.* **85**, 4988 (2000).

- [10] M. Peyrard and A.R. Bishop, *Phys. Rev. Lett.* **62**, 2755 (1989).
- [11] L. D. Landau and E. M. Lifshitz, *Quantum Mechanics*, Pergamon (1977).
- [12] A related instability is the wetting of interfaces, where many of the ideas discussed here have been developed, cf. D. M. Kroll and R. Lipowski, *Phys. Rev. B* **28**, 5273 (1983), R. Lipowski, *Phys. Rev. B* **32**, 1731 (1985).
- [13] T. Dauxois, M. Peyrard and A. R. Bishop, *Phys. Rev. E* **47**, R4 (1993).
- [14] T. Dauxois and M. Peyrard, *Phys. Rev. E* **51**, 4027 (1995).
- [15] N. Theodorakopoulos, T. Dauxois and M. Peyrard, *Phys. Rev. Lett.* **85**, 6 (2000).
- [16] R. K. P. Zia, R. Lipowski and D. M. Kroll *Am. J. Phys.* **56**, 160 (1988); N.Theodorakopoulos (unpublished).
- [17] D. Cule and T. Hwa, *Phys. Rev. Lett.* **79**, 2375 (1997).
- [18] Y-L Zhang, W-M Zheng, J-X Liu, Y. Z. Chen, *Phys. Rev. E* **56**, 7100 (1997).
- [19] N. Theodorakopoulos (to be published).
- [20] T. Dauxois, N. Theodorakopoulos and M. Peyrard, *J. Stat. Phys.* **107**, 869 (2002).
- [21] L. van Hove, *Physica* **16**, 137 (1950).
- [22] J.A. Cuesta and A. Sanchez, *J. Phys. A: Math. Gen.* **35**, 2373 (2002).
- [23] L. D. Landau and E. M. Lifshitz, *Statistical Physics*, Pergamon (1980).